Inorganica Chimica Acta 389 (2012) 168–175

Contents lists available at SciVerse ScienceDirect

Inorganica Chimica Acta

journal homepage: www.elsevier.com/locate/ica

Small molecule inhibitors of PSMA incorporating technetium-99m for imaging prostate cancer: Effects of chelate design on pharmacokinetics

Kevin P. Maresca, Shawn M. Hillier, Genliang Lu, John C. Marquis, Craig N. Zimmerman, William C. Eckelman, John L. Joyal, John W. Babich *

Molecular Insight Pharmaceuticals, Inc., 160 Second Street, Cambridge, MA 02142, United States

ARTICLE INFO

Article history:
Available online 10 March 2012

Dedicated to Prof. Jon Zubieta

Keywords:
Technetium-99m
Tc-tricarbonyl
SAAC II
PSMA inhibitors
Chelates

ABSTRACT

Single amino acid chelate (SAAC) systems for the complexation of the $M(CO)_3$ moiety (M = Tc/Re) have been successfully incorporated into novel synthetic strategies for radiopharmaceuticals and evaluated in a variety of biological applications. However, the lipophilicity of the first generation of $^{99m}Tc(CO)_3$ complexes has resulted in substantial hepatobiliary uptake when examined either as lysine derivatives or integrated into biologically active small molecules and peptides. Here, we designed, synthesized, and evaluated novel polar functionalized imidazole derived SAAC systems (SAAC II) which have been chemically modified to promote overall $^{99m}Tc(CO)_3L_3$ complex hydrophilicity with the intent of reducing non-target effects and enhancing renal clearance of prostate specific membrane antigen (PSMA) targeting small molecules. The ^{99m}Tc-labeled compounds were prepared, purified, and evaluated for stability, lipophilicity, and tissue distribution in LNCaP xenograft mice. The Glu-urea-Lys-C11 analogs were prepared with a variety of chelators to form (19*R*,23*S*)-1-(**X**)-2-((**Y**)methyl)-13,21-dioxo-2,14,20,22-tetraazapentacosane-19,23,25-tricarboxylic acid where X = Y = (methyl)pyridin-2-yl (**6**), X = Y = (methyl)-1*H*-imidazol-2-yl (**7**), X = (methyl)pyridin-2-yl, Y = carboxymethyl (**8**), X = Y = 1-(carboxymethyl)-1*H*-imidazol-2-yl (**9**), X = 1-(carboxymethyl)-1*H*-imidazol-2-yl, Y = carboxymethyl (**10**), and X = Y = 1-(1-(2-(bis(carboxymethyl)amino)-2-oxoethyl)-1H-imidazol-2-yl)-2-((1-(2-(bis(carboxymethyl)amino)-2-oxoethyl)-1H-imidazol-2-yl) (**11**). ^{99m}Tc labeling was achieved at ligand concentrations as low as 10^{-6} M and the complexes were stable (>90%) for 24 h. These new SAAC II chelators were evaluated for their influence on binding of the Glu-urea-Lys-C11 analogs to PSMA-positive LNCaP cells and compared to pyridine- and *N*-methylimidazole-containing SAAC ligands. Tissue distribution of the ^{99m}Tc-complexes containing the more polar chelators, **9** and **11**, demonstrated decreased liver (<2% ID/g) and increased LNCaP tumor (>11% ID/g) accumulation at 1 h post-injection.

1. Introduction

Metals have been used in medicine for radiodiagnostic and radiotherapeutic applications for decades [1–3]. Of all the radiometals used in medicine today none has more prominence than the transition metal, technetium, specifically the radionuclide Tc-99m [4]. Tens of millions of imaging procedures are performed annually worldwide using this radiometal attached to a variety of mostly organic ligands that influence the biological fate and protein interactions of the metal–ligand complex *in vivo*, thereby creating scintigraphic images that allow physicians to infer diagnostic information based on morphology and function [1,5].

The polyvalent nature of Tc demands that due consideration is given to the chemical approach used for its incorporation into a targeting ligand. How the metal is bound can greatly influence the overall pharmacological character and biological fate of the complex, by altering the overall charge, polarity, hydrophobicity, and steric bulk. As the size of the structural moiety responsible for biological targeting decreases the influence of the metal-complex generally increases, such that large proteins like immunoglobulins would be considerably less affected by the presence and nature of a metal–chelate structure than smaller molecules (such as an enzyme inhibitor or peptide) used for imaging biological targets such as enzymes or receptors. It is therefore reasonable to conclude that the chelate, the metal–chelate complex and the nature of the outer solvation sphere of the metal chelate complex all directly or indirectly influence the performance of such a radiolabeled ligand in regards to its intended pharmacological and clinical purpose [6–11].

We have previously described a chelate platform incorporating the epsilon amine of lysine as one of three donor atoms in a tridentate chelate system, referred to as single amino acid chelate (SAAC) [12,13]. This amino acid based radiolabeling platform is

* Corresponding author.
E-mail address: jbabich@molecularinsight.com (J.W. Babich).

0020-1693/$ - see front matter © 2012 Elsevier B.V. All rights reserved.
http://dx.doi.org/10.1016/j.ica.2012.03.002

constructed from derivatized amino acids modified to provide three donor groups (L_3) for chelation to the $\{M(CO)_3\}^{+1}$ core (M = ^{99m}Tc or Re), as described by Alberto and co-workers [14,15]. SAAC, as exemplified by 2-amino-6-(bis-pyridin-2-yl-methyl-amino)-hexanoic acid, (dipyridyl-lysine or DPK), demonstrated facile radiolabeling with $\{^{99m}Tc(CO)_3\}^{+1}$ and robust stability of the formed complex [16,17]. In addition, SAAC ligands, like DPK, may be incorporated into bioactive peptides via standard solid phase peptide synthesis as the non-radioactive Re complex ($\{M(CO)_3L_3\}^{+1}$) or as the free ligand which is subsequently labeled with ^{99m}Tc or $^{186/188}$Re [18,19]. However, our experience to date has shown that the hydrophobic nature of the dipyridyl metal complexes has a powerful and unwanted affect on *in vivo* pharmacokinetics. We have recently shown that altering the nitrogen containing ring structures of SAAC from pyridyl groups to functionalized imidazolyl groups incorporating polar, hydrophilic groups such as carboxylates can significantly reduce this affect on peptide receptor targeting ligands such as octreotide [20].

Here, we describe the synthesis of a series of SAAC containing glutamate-urea-lysine (Glu-urea-Lys) derivatives, for targeting PSMA, with a variety of metal donor ligand groups to form (19*R*,23*S*)-1-(**X**)-2-((**Y**)methyl)-13,21-dioxo-2,14,20,22-tetraazapentacosane-19,23,25-tricarboxylic acid where **X** = **Y** = (methyl)pyridin-2-yl (**6**), X = Y = (methyl)-1*H*-imidazol-2-yl (**7**), X = (methyl)pyridin-2-yl, Y = carboxymethyl (**8**), X = Y = 1-(carboxymethyl)-1*H*-imidazol-2-yl (**9**), X = 1-(carboxymethyl)-1*H*-imidazol-2-yl, Y = carboxymethyl (**10**), and X = Y = 1-(1- (2 -(bis(carboxymethyl)amino)-2-oxoethyl)-1*H*-imida .3zol-2-yl)-2-(1-(2-(bis(carboxymethyl)amino)-2-oxoethyl)-1*H*-imidazol-2-yl) (**11**). The ^{99m}Tc/Re complexes of these Glu-urea-Lys-C11-SAAC ligands were then prepared and evaluated to determine the influence the chelators had on the *in vitro* target affinity, and *in vivo* tumor localization and normal organ tissue distribution in nude mice bearing human prostate cancer xenografts.

2. Experimental

2.1. General methods

All reactions were carried out in dry glassware under an atmosphere of argon unless otherwise noted. Reactions were purified by column chromatography under medium pressure using a Biotage SP4 or by semi-preparative high pressure liquid chromatography using a Varian Prostar 210 high pressure liquid chromatography (HPLC) system equipped with a semi-preparative Vydac C18 reverse-phase column (250 mm × 10 mm × 5 μm) connected to a Varian Prostar model 320 UV–Vis detector and monitored at a wavelength of 254 nm. The final technetium complexes were purified and analyzed using a binary solvent gradient of 5–95% buffer B over 21 min (buffer A = triethylammonium phosphate (TEAP), pH 3), (buffer B = methanol) or were purified and analyzed with a Vydac C18 reverse phase column (250 mm × 4.6 mm × 5 μm) employing a gradient method of 5–50% buffer B over 30 minutes (buffer A = water + 0.1% TFA, buffer B = acetonitrile + 0.1% TFA). ^{1}H NMR spectra were obtained on a Bruker 400 MHz instrument. Spectra are reported as δ (ppm) and are referenced to the solvent resonances in chloroform-*d* ($CDCl_3$), dimethylsulfoxide-d_6 (DMSO-d_6) or methanol-d_4 (MeOD). ^{99m}Tc was obtained from a commercial ^{99}Mo/^{99m}Tc generator eluant (Cardinal Health) and was used as a solution of $Na^{99m}TcO_4$ in saline. The ^{99m}Tc containing solutions are kept behind a lead shield that offers sufficient protection. The $[^{99m}Tc(CO)_3(H_2O)_3]^+$ utilized in the formation of the ^{99m}Tc complexes was prepared from commercially available Isolink™ kits (Mallinckrodt/Covidien). Solvents and reagents were purchased from Sigma Aldrich (St. Louis, MO), Bachem (Switzerland), Akaal (Long Beach, CA), or Anaspec (San Jose, CA) unless otherwise noted. The following common abbreviations are used: AcOH = acetic acid, DMF = *N*,*N*-dimethylformamide, DMSO = dimethylsulfoxide, DCM = dichloromethane, DCE = 1,2-dichloroethane, Glu = glutamic acid, NaOH = sodium hydroxide, HATU = 2-(7-aza-1*H*-benzotriazole-1-yl)-1,1,3,3-tetramethyluronium hexafluorophosphate, $NaBH(OAc)_3$ = sodium triacetoxyborohydride, EtOAc = ethyl acetate, TEA = triethylamine, DIPEA = diisopropylethyl amine, ID/g = injected dose per gram, PBS = phosphate buffered saline, RCP = radiochemical purity.

2.2. Synthesis

2.2.1. General procedure for the alkylations

To a solution of the imidazole-2-carboxaldehyde dissolved in DMF (1 mL) was added 1 mol equivalent of the alkylbromide, excess potassium carbonate and a catalytic amount of potassium iodide. The reactions were heated at 110 °C for 18 h followed by evaporation to dryness and purified utilizing a Biotage SP4 with a gradient method of 5–50% methanol in DCM.

2.2.2. General procedure for the reductive aminations

To a solution of 1-amino undecanoic acid dissolved in DCE (2 mL) was added 2.1 equivalence of the aldehyde. The reaction was heated at 50 °C for one hour whereupon 2 equivalents of sodium triacetoxyborohydride was added. The reaction stirred at room temperature for 12 h and was subsequently evaporated to dryness and purified using a Biotage SP4 with a gradient method of 5–50% methanol in DCM afforded the desired compounds.

2.2.3. General synthesis of Glu-urea-Lys(X) analogs

The compounds (**6**, **7** and **9**–**11**) of the general structure **5** were prepared in overall yields ranging from 10% to 50% using the general route depicted in Scheme 1. The key synthetic intermediate for all the compounds was formed by reacting the appropriate aldehyde at room temperature for 1 h to form the schiff base intermediate. The schiff base was not isolated but was reduced *in situ* with sodium triacetoxyborohydride to form the bis-derivatized amine (**2**). The derivatized amine was coupled to (*S*)-di-*tert*-butyl-2-(3-((*S*)-6-amino-1-(*tert*-butoxy)-1-oxohexan-2-yl)ureido)pentanedioate (**1**) using the terminal carboxylic acid, HATU and base to form the protected intermediate **3**. The synthesis of the Re(I) complexes (**4**) was accomplished by the reaction of $[NEt_4]_2[ReBr_3(CO)_3]$ with the appropriate ligand in the ratio of 1:1.2 in 10 mL of methanol. The reaction was heated at 80 °C for 4 h. Upon cooling the reaction products were purified using C18 Sep Pak columns with yields ranging from 20-50%. The *tert*-butyl ester protecting groups were removed with 50% TFA in DCM after 12 h at room temperature. Upon completion of the deprotection, the reactions were concentrated on a rotary evaporator and purified by HPLC or flash chromatography to afford the desired products (**5**) in 10–50% yield.

2.2.4. (19*R*,23*S*)-tri-tert-butyl-13,21-dioxo-1-(pyridin-2-yl)-2-(pyridin-2-ylmethyl)-2,14,20,22-tetraazapentacosane-19,23,25-tricarboxylate (**6**)

The (19*R*,23*S*)-tri-*tert*-butyl-13,21-dioxo-1-(pyridin-2-yl)-2-(pyridin-2-ylmethyl)-2,14,20,22-tetraazapentacosane-19,23,25-tricarboxylate (**6**) was prepared following the same general procedure as shown in Scheme 1, using previously prepared and protected (*S*)-di-*tert*-butyl-2-(3-((*S*)-6-amino-1-(*tert*-butoxy)-1-oxohexan-2-yl)ureido)pentanedioate (**1**). The reaction mixture was purified by reverse phase HPLC 10–100% buffer B in buffer A as eluent to afford **6** (151 mg, 0.17 mmol, 11%) as a white solid. ^{1}H NMR (400 MHz, DMSO-d_6) δ 8.47 (dd, 2H), 7.81 (m, 2H), 7.70 (s, 1H), 7.45 (m, 2H), 7.37 (m, 2H), 6.25 (m, 2 H), 4.25 (m, 2H), 3.95 (s, 4H), 2.98 (m, 2H), 2.30 (m, 2 H), 2.20 (m, 4H), 2.05 (m, 2H), 1.90 (m, 2H), 1.60 (m, 4H), 1.38 (s, 27H), 1.20 (m, 16 H); MS (ESI): 854$(M+H)^+$.

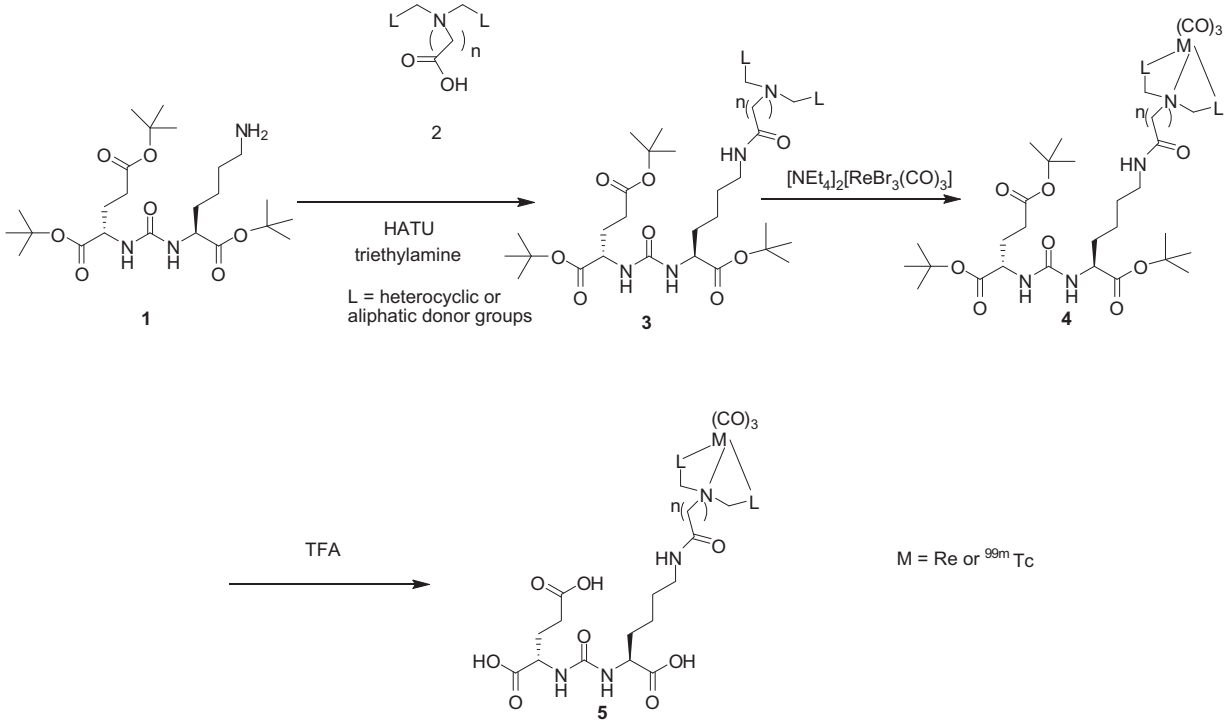

Scheme 1. General pathway for the synthesis of ^{99m}Tc or Re-Glu-urea-Lys-X analogs (**5**).

*2.2.5. [Re(CO)$_3$\{((19R,23S)-13,21-dioxo-1-(pyridin-2-yl)-2-(pyridin-2-ylmethyl)-2,14,20,22-tetraazapentacosane-19,23,25-tricarboxylic acid\}] (**6R**)*

The rhenium complex was prepared following the same procedure as described in the general rhenium experimental methods using **6** to yield the desired product **6R** (6 mg, 0.0063 mmol, 7.4%) as an off-white solid. ^{1}H NMR (400 MHz, d_6-DMSO) δ 8.77 (dd, 2H), 7.98 (t, 2H), 7.70 (s, H), 7.47 (d, 2H), 7.38 (m, 2 H), 6.25 (m, 2H), 4.84 (m, 2H), 3.75 (m, 4H), 3.0 (m, 2H), 2.25 (m, 2H), 2.20 (m, 4H), 2.05 (m, 2H), 1.85 (m, 2H), 1.55 (m, 4H), 1.22 (m, 16 H); MS (ESI): 955 (M+H)$^+$.

*2.2.6. (19R,23S)-tri-tert-butyl-1-(1-methyl-1H-imidazol-2-yl)-2-((1-methyl-1H-imidazol-2-yl)methyl)-13,21-dioxo-2,14,20,22-tetraazapentacosane-19,23,25-tricarboxylate (**7**)*

(19*R*,23*S*)-tri-*tert*-butyl-1-(1-methyl-1*H*-imidazol-2-yl)-2-((1-methyl-1*H*-imidazol-2-yl)methyl)-13,21-dioxo-2,14,20,22-tetraazapentacosane-19,23,25-tricarboxylate (**7**) was prepared following the same general procedure as shown in Scheme 1, using previously prepared and protected (*S*)-di-*tert*-butyl-2-(3-((*S*)-6-amino-1-(*tert*-butoxy)-1-oxohexan-2-yl)ureido)pentanedioate (**1**). The reaction mixture was purified by use of a Biotage SP4 purification system with a gradient of 5–50% methanol in DCM as eluent to afford **7** (57 mg, 0.066 mmol, 9%) as a white solid. ^{1}H NMR (400 MHz, DMSO-d_6) δ 7.70 (s, H), 7.10 (d, 2 H), 6.84 (d, 2H), 6.23 (m, 2H), 4.00 (m, 2H), 3.6 (s, 2H), 3.44 (s, 2 H), 3.07 (s, 6H), 3.02 (m, 2H), 2.39 (t, 2H), 2.24 (m, 4H), 2.05 (t, 2H), 1.60 (m, 4H), 1.35 (s, 27H), 1.15 (m, 16H); MS (ESI): 860(M+H)$^+$.

*2.2.7. [Re(CO)$_3$\{(19R,23S)-1-(1-methyl-1H-imidazol-2-yl)-2-((1-methyl-1H-imidazol-2-yl)methyl)-13,21-dioxo-2,14,20,22-tetraazapentacosane-19,23,25-tricarboxylic acid\}] (**7R**)*

The rhenium complex was prepared following the same procedure as described in the general rhenium experimental methods to yield the desired product **7R** (3.2 mg, 0.003 mmol, 5.2%) as an off-white solid. ^{1}H NMR (400 MHz, DMSO-d_6) δ 7.70 (s, H), 7.10 (d, 2 H), 7.03 (d, 2H), 6.33 (m, 2H), 5.72 (s, 4H), 4.60 (dd, 4H), 4.00 (m, 2H), 3.6 (s, 6H), 2.98 (d, 2H), 2.26 (m, 2H), 2.39 (t, 2H), 2.24 (m, 4H), 2.01 (t, 4H), 1.83 (m, 2H), 1.60–1.35 (m, 4H), 1.30 (m, 16H); MS (ESI): 962 (M+H)$^+$.

*2.2.8. (19R,23S)-13,21-dioxo-2-(pyridin-2-ylmethyl)-2,14,20,22-tetraazapentacosane-1,19,23,25-tetracarboxylic acid (**8**)*

The (19*R*,23*S*)-13,21-dioxo-2-(pyridin-2-ylmethyl)-2,14,20,22-tetraazapentacosane-1,19,23,25-tetracarboxylic acid (**8**) was prepared employing the same general procedure as shown in Scheme 1, using previously prepared and protected (*S*)-di-tert-butyl-2-(3-((*S*)-6-amino-1-(*tert*-butoxy)-1-oxohexan-2-yl)ureido)-pentanedioate (**1**). The reaction mixture was purified by Biotage SP4 with a gradient method of 5–50% methanol in DCM as eluent to afford **8** (3 mg, 0.005 mmol, 9%) as a white solid. ^{1}H NMR (400 MHz, DMSO-d_6) δ 8.45 (d, H), 7.95 (t, H), 7.75 (m, 2H), 7.65 (m, 2H), 6.40 (m, 2H), 4.60 (m, 2H), 4.05 (s, 2H), 3.62 (s, 2H), 3.0 (m, 2H), 2.65 (m, 2H), 2.30 (m, 2H), 2.15 (m, 4H), 1.98 (m, 2H), 1.50 (m, 4H), 1.3 (m, 16H); MS (ESI): 652 (M+H)$^+$.

*2.2.9. [Re(CO)$_3$\{(19R,23S)-13,21-dioxo-2-(pyridin-2-ylmethyl)-2,14,20,22-tetraazapentacosane-1,19,23,25-tetracarboxylic acid\}] (**8R**)*

The rhenium complex was prepared employing the same procedure as described in the general rhenium experimental. The compound was deprotected using the previously described methods to yield the desired product **8R** (3.0 mg, 0.003 mmol, 75%) as an off-white solid. MS (ESI): 922 (M+H)$^+$.

*2.2.10. (19R,23S)-tri-tert-butyl-1-(1-(2-tert-butoxy-2-oxoethyl)-1H-imidazol-2-yl)-2-((1-(2-tert-butoxy-2-oxoethyl)-1H-imidazol-2-yl)methyl)-13,21-dioxo-2,14,20,22-tetraazapentacosane-19,23,25-tricarboxylate (**9**)*

The (19*R*,23*S*)-tri-*tert*-butyl-1-(1-(2-*tert*-butoxy-2-oxoethyl)-1*H*-imidazol-2-yl)-2-((1-(2-*tert*-butoxy-2-oxoethyl)-1*H*-imidazol-2-yl)methyl)-13,21-dioxo-2,14,20,22-tetraazapentacosane-19,23,

25-tricarboxylate was prepared following the same general procedure as shown in Scheme 1, using previously prepared and protected (*S*)-di-tert-butyl-2-(3-((*S*)-6-amino-1-(tert-butoxy)-1-oxohexan-2-yl)ureido)pentanedioate (**1**) to afford **9** (234 mg, 0.22 mmol, 61%) as a white solid. ^{1}H NMR (400 MHz, DMSO-d_6) δ 8.25 (s, 1H), 7.20 (s, 2H), 6.95 (s, 2H), 6.22 (m, 2H), 4.80 (d, 4H), 4.11 (m, 2H), 3.80 (s, 4H), 2.99 (m, 2H), 2.46 (m, 2H), 2.30 (m, 4H), 2.1 (m, 2H), 1.90 (m, 2H), 1.55 (m, 4H), 1.30 (s, 45H), 1.2 (m, 16H). MS (ESI): 530(M/2).

2.2.11. [Re(CO)$_3$(19R,23S)-1-(1-(carboxymethyl)-1H-imidazol-2-yl)-2-((1-(carboxymethyl)-1H-imidazol-2-yl)methyl)-13,21-dioxo-2,14,20,22-tetraazapentacosane-19,23,25-tricarboxylic acid}] (**9R**)

The rhenium complex was prepared employing the same procedure as described in the general rhenium experimental to yield the desired product **9R** (7.0 mg, 0.006 mmol, 24%) as an off-white solid. ^{1}H NMR (400 MHz, DMSO-d_6) δ 7.8 (s, H), 7.2 (s, 2H), 7.0 (2, 2H), 6.3 (s, 2H), 4.8 (s, 4H), 4.55 (d, 2H), 4.1 (m, 4H), 2.9 (m, 2H), 2.2 (m, 4H), 2.05 (m, 4H), 1.7 (m, 2H), 1.45 (m, 4H), 1.3 (m, 16H); MS (ESI): 525 (M/2).

2.2.12. (19S,23S)-tetra-tert-butyl-2-((1-(2-tert-butoxy-2-oxoethyl)-1H-imidazol-2-yl)methyl)-13,21-dioxo-2,14,20,22-tetraazapentacosane-1,19,23,25-tetracarboxylate (**10**)

A suspension of 11-aminoundecanoic acid (603 mg, 3.0 mmol), 2-pyridinecarboxaldehyde (630 mg, 3.0 mmol) and AcOH (0.20 mL) in DCE (20 mL) was heated to reflux for 30 min. The reaction mixture was cooled to 0 °C, and treated sequentially with NaBH(OAc)$_3$ (1.9 g, 9.0 mmol) and crude *tert*-butyl glyoxalate (1.50 g, 11.5 mmol). The reaction mixture was stirred at room temperature for overnight and decomposed with water. The reaction mixture was extracted with DCM. The organic layer was dried and concentrated under reduced pressure. The residue was purified by Biotage SP4 5-50% methanol in DCM as eluent to afford 11-((2-*tert*-butoxy-2-oxoethyl)((1-(2-*tert*-butoxy-2-oxoethyl)-1*H*-imidazol-2-yl)methyl)amino)undecanoic acid (343 mg, 0.67 mmol, 22%) as a yellow oil. ^{1}H NMR (400 MHz, CDCl$_3$) δ 7.00 (d, 1H), 6.87 (d, 1H), 5.30 (s, 1H), 5.07 (s, 1H), 4.67 (s, 2H), 4.66 (s, 2H), 3.83 (s, 1H), 3.17 (s, 1H), 2.41–2.32 (m, 2H), 1.66–1.63 (m, 2H), 1.47 (s, 9H), 1.45 (s, 9H), 1.42–1.10 (m, 14H); MS (ESI): 510 (M+H)$^+$.

2.2.13. Step 2. (19S,23S)-tetra-tert-butyl-2-((1-(2-tert-butoxy-2-oxoethyl)-1H-imidazol-2-yl)methyl)-13,21-dioxo-2,14,20,22-tetraazapentacosane-1,19,23,25-tetracarboxylate

A solution of (*S*)-di-tert-butyl-2-(3-((*S*)-6-amino-1-(*tert*-butoxy)-1-oxohexan-2-yl)ureido)pentanedioate (**1**) (85 mg, 0.175 mmol), 11-((2-*tert*-butoxy-2-oxoethyl)((1-(2-*tert*-butoxy-2-oxoethyl)-1*H*-imidazol-2-yl)methyl)amino)undecanoic acid (89 mg, 0.175 mmol), EDCI (38 mg, 0.20 mmol), HOBt (26 mg, 0.20 mmol) and DIPEA (0.30 mL) in DCM (5.0 mL) was stirred at rt for 3 days. The reaction mixture was purified by Biotage SP4 5–50% methanol in DCM as eluent to afford (19*S*,23*S*)-tetra-*tert*-butyl-2-((1-(2-*tert*-butoxy-2-oxoethyl)-1*H*-imidazol-2-yl)methyl)-13,21-dioxo-2,14,20,22-tetraazapentacosane-1,19,23,25-tetracarboxylate (111 mg, 0.11 mmol, 65%) as a yellow oil. MS (ESI): 490.5 (M/2+H)$^+$.

2.2.14. [Re(CO)$_3${(19R,23S)-2-((1-(carboxymethyl)-1H-imidazol-2-yl)methyl)-13,21-dioxo-2,14,20,22-tetraazapentacosane-1,19,23,25-tetracarboxylic acid}] (**10R**)

A solution of (19*S*,23*S*)-tetra-*tert*-butyl-2-((1-(2-*tert*-butoxy-2-oxoethyl)-1*H*-imidazol-2-yl)methyl)-13,21-dioxo-2,14,20,22-tetraaza penta cosane-1,19,23,25-tetracarboxylate (18.8 mg, 0.019 mmol) in TFA (1.0 mL)/DCM (1.0 mL) was stirred at room temperature overnight. The solvent was evaporated to give (19*S*,23*S*)-2-((1-(carboxymethyl)-1*H*-imidazol-2-yl)methyl)-13,21-dioxo-2,14,20,22-tetraazapentacosane -1,19,23,25-tetracarboxylic acid as a colorless oil. To a solution of the above deprotected product in water (1.0 mL) that was adjusted to pH 9 with 2 N NaOH was added Re(CO)$_3$(H$_2$O)OTf (0.50 mL, 0.10 mL/mmol). The reaction mixture were stirred at room temperature overnight and purified by HPLC 10–100% buffer B buffer in buffer A as eluent to afford **10R** (4.0 mg, 0.004 mmol, 19%) as a white solid. ^{1}H NMR (400 MHz, DMSO-d_6) δ 7.70 (t, 1H), 7.33 (s, 1H), 7.13 (s, 2H), 6.29 (d, 1H), 6.26 (d, 1H), 4.96 (d, 2H), 4.56 (d, 1H), 4.12 (d, 1H), 4.07–3.90 (m, 2H), 3.70 (d, 1H), 3.40 (d, 1H), 2.98–2.94 (m, 4H), 2.21 (q, 2H), 1.99 (t, 2H), 1.70–1.22 (m, 24H); MS (ESI): 485.2 (M/2+H)$^+$.

2.2.15. (19S,23S)-tri-tert-butyl-1-(1-(2-(bis(2-tert-butoxy-2-oxoethyl) amino)-2-oxoethyl)-1H-imidazol-2-yl)-2-((1-(2-(bis(2-tert-butoxy-2-oxo ethyl)amino)-2-oxoethyl)-1H-imidazol-2-yl)methyl)-13,21-dioxo-2,14, 20,22-tetraazapentacosane-19,23,25-tricarboxylate (**11**)

(19*S*,23*S*)-1-(1-(2-(bis(carboxymethyl)amino)-2-oxoethyl)-1*H*-imidazol-2-yl)-2-((1-(2-(bis(carboxymethyl)amino)-2-oxoethyl)-1*H*-imidazol-2-yl)methyl)-13,21-dioxo-2,14,20,22-tetraazapentacosane-19, 23, 25-tr icarboxylic acid was prepared following the same general procedure as shown in Scheme 1, using previously prepared and protected (*S*)-di-tert-butyl-2-(3-((*S*)-6-amino-1-(tert-butoxy)-1-oxohexan-2-yl)ureido) pentanedioate (**1**).

2.2.16. Step 1. tert-butyl-2,2′-(2-bromoacetylazanediyl)diacetate

To a solution of *tert*-butyl-2,2′-azanediyldiacetate (3.00 g, 12.24 mmol) and 2-bromoacetyl bromide (3.23 g, 1.39 mL, 16.00 mmol) in DCM (100 mL) was added TEA (2.0 mL) at room temperature. The reaction mixture was stirred at room temperature for 2 h then diluted with DCM (300 mL), washed with water, and dried over sodium sulfate. Solvent was evaporated under reduce pressure to afford a residue, which was purified by biotage eluting with 10% hexanes in EtOAc to 50% hexanes in EtOAc to tert-butyl-2,2′-(2-bromoacetylazanediyl)diacetate (4.68 g, 100%). ^{1}H NMR (400 MHz, CDCl$_3$) δ 4.09 (s, 2H), 4.07 (s, 2H), 3.86 (s, 2H), 1.49 (s, 9H), 1.46 (s, 9H); MS (ESI): 388, 390 (M+Na)$^+$.

2.2.17. Step 2. tert-butyl-2,2′-(2-(2-formyl-1H-imidazol-1-yl)acetylazanediyl)diacetate

A solution of *tert*-butyl-2,2′-(2-bromoacetylazanediyl)diacetate (4.55 g, 12.43 mmol), 1*H*-imidazole-2-carbaldehyde (1.54 g, 16.0 mmol), DIPEA (5.0 mL), and potassium iodide (0.64 g, 4.0 mmol) was stirred at 80 °C overnight. The solvent was evaporated under reduced pressure, the reaction mixture was diluted with DCM, washed with water and dried. The solvent was evaporated under reduce pressure to afford a residue, which was purified by Biotage SP4 DCM to 3% MeOH in DCM as eluent to afford the desired product *tert*-butyl-2,2′-(2-(2-formyl-1*H*-imidazol-1-yl)acetylazanediyl)diacetate (3.96 g, 84%). ^{1}H NMR (400 MHz, CDCl$_3$) δ 9.76 (s, 1H), 7.31 (s, 1H), 7.25 (s, 1H), 5.30 (s, 2H), 4.14 (s, 2H), 4.07 (s, 2H), 1.51 (s, 9H), 1.43 (s, 9H); MS (ESI): 382 (M+H)$^+$.

2.2.18. Step 3. 11-(bis((1-(2-(bis(2-tert-butoxy-2-oxoethyl)amino)-2-oxoethyl)-1H-imidazol-2-yl)methyl)amino)undecanoic acid

A solution of 11-aminoundecanoic acid (100 mg, 0.50 mmol), *tert*-butyl-2,2′-(2-(2-formyl-1H-imidazol-1-yl)acetylazanediyl) diacetate (381 mg, 1.0 mmol) and AcOH (0.02 mL) in DCE (30 mL) was stirred at 75 °C for 30 min under nitrogen. The reaction mixture was cooled to 0 °C, and treated with NaBH(OAc)$_3$ (0.3165 g, 1.5 mmol). The reaction mixture was stirred at room temperature overnight and decomposed with water. The solvent was evaporated under reduce pressure to afford a residue, which was purified by Biotage SP4 1–10% MeOH in DCM as eluent to afford the desired product 11-(bis((1-(2-(bis(2-*tert*-butoxy-2-oxoethyl)amino)-2-oxo ethyl)-1*H*-imidazol-2-yl)methyl)amino)undecanoic acid (368 mg, 79%). ^{1}H NMR (400 MHz, DMSO-d_6) δ 6.93 (s, 2H), 6.76 (s, 2H), 5.02 (s, 4H), 4.29 (s, 4H), 3.93 (s, 4H), 3.44 (s, 4H), 2.30 (t,

J = 7.6 Hz, 2H), 2.09 (t, J = 7.6 Hz, 2H), 1.43 (s, 18H), 1.35 (s, 18H), 1.29–1.00 (m, 16H); MS (ESI): 466.9 $(M/2+H)^+$.

2.2.19. Step 4. (19S,23S)-tri-tert-butyl-1-(1-(2-(bis(2-tert-butoxy-2-oxoethyl)amino)-2-oxoethyl)-1H-imidazol-2-yl)-2-((1-(2-(bis(2-tert-butoxy-2-oxoethyl)amino)-2-oxoethyl)-1H-imidazol-2-yl)methyl)-13,21-dioxo-2,14,20,22-tetraazapentacosane-19,23,25-tricarboxylate

A solution of (*S*)-di-tert-butyl-2-(3-((*S*)-6-amino-1-(tert-butoxy)-1-oxohexan-2-yl)ureido)pentanedioate (**1**) (85 mg, 0.174 mmol), 11-(bis((1-(2-(bis(2-tert-butoxy-2-oxoethyl)amino)-2-oxoethyl)-1*H*-imidazol-2-yl)methyl)amino)undecanoic acid (118 mg, 0.127 mmol), EDC (38 mg, 0.20 mmol), HOBt (26 mg, 0.20) and DIPEA (0.30 mL) in DCM (5.0 mL) was stirred at rt overnight. The reaction mixture was purified by Biotage SP4 1–10% MeOH in DCM as eluent to afford (19*S*,23*S*)-tri-*tert*-butyl-1-(1-(2-(bis(2-*tert*-butoxy-2-oxoethyl)amino)-2-oxoethyl)-1*H*-imidazol-2-yl)-2-((1-(2-(bis(2-*tert*-butoxy-2-oxoethyl)amino)-2-oxoethyl)-1*H*-imidazol-2-yl)methyl)-13,21-dioxo-2,14,20,22-tetraaza pentacosane-19,23,25-tricarboxylate (38 mg, 0.03 mmol, 21%) as a colorless oil. ^{1}H NMR (400 MHz, $CDCl_3$) δ 6.95 (d, J = 1.2 Hz, 2H), 6.83 (d, J = 0.80 Hz, 2H), 5.97 (s, 1H), 5.28 (d, J = 7.6 Hz, 1H), 5.23 (d, J = 8.4 Hz, 1H), 4.94 (s, 4H), 4.33–4.25 (m, 2H), 4.12 (s, 4H), 4.03 (s, 4H), 3.63 (s, 4H), 3.25–3.16 (m, 2H), 2.53 (t, J = 7.4 Hz, 2H), 2.33–2.24 (m, 2H), 2.15 (t, J = 7.6 Hz, 2H), 2.08–2.03 (m, 2H), 2.02–1.20 (m, 85H); MS (ESI): 701.6 $(M/2+H)^+$.

*2.2.20. [Re(CO)$_3${(19S,23S)-1-(1-(2-(bis(carboxymethyl)amino)-2-oxoethyl)-1H-imidazol-2-yl)-2-((1-(2-(bis(carboxymethyl)amino)-2-oxoethyl)-1H-imidazol-2-yl)methyl)-13,21-dioxo-2,14,20,22-tetraazapentacosane-19,23,25-tricarboxylic acid}] (**11R**)*

The rhenium complex was prepared following the same procedure as described in the general rhenium experimental to yield the desired product (17.6 mg, 0.014 mmol, 69% over 2 steps) as a white solid. ^{1}H NMR (400 MHz, DMSO-d_6) δ 7.70 (t, J = 4.8 Hz, 1H), 7.10 (s, 2H), 7.03 (s, 2H), 6.29 (d, J = 8.4 Hz, 1H), 6.26 (d, J = 8.4 Hz, 1H), 5.02 (s, 4H), 4.37–3.97 (m, 14H), 3.60–3.57 (m, 2H), 3.01–2.94 (m, 2H), 2.24–1.22 (m, 28H); MS (ESI): 640.3 $(M/2+H)^+$.

2.3. In vitro screening

LNCaP human prostate cancer cells were obtained from American Type Culture Collection, Rockville, MD, and maintained in RPMI-1640 medium supplemented with 10% fetal bovine serum (FBS). Competitive binding of the cold Re derivatives to LNCaP cells was performed as previously described [21]. Briefly, cells were plated in 12-well plates at approximately 4×10^5 cells/well and incubated for 48 h in a humidified incubator at 37 °C/5% carbon dioxide prior to addition of compound. Each Glu-urea-X derivative was prepared and diluted in serum-free cell culture medium containing 0.5% bovine serum albumin (BSA) in combination with 3 nM ^{123}I-(*S*)-2-(3-((*S*)-1-carboxy-5-(4-iodobenzylamino)pentyl)ureido)-pentanedioic acid (MIP-1072) or *N*-[*N*-[(*S*)-1,3-dicarboxypropyl]carbamoyl]-*S*-3-iodo-L-tyrosine (^{123}I-DCIT). Plates were incubated at room temperature for 1 h. Cells were removed from the plates by gently pipeting and transferred to eppendorff tubes. Samples were microcentrifuged for 15 s at 10 K × g. The medium was aspirated and the pellet was washed twice by dispersal in fresh assay medium followed by microcentrifugation. Cell binding of ^{123}I-(*S*)-2-(3-((*S*)-1-carboxy-5-(4-iodobenzylamino)pentyl) ureido)pentanedioic acid or ^{123}I-DCIT was determined by counting the cell pellet in an automated gamma counter.

2.4. General preparation of ^{99m}Tc-complexes

The ^{99m}Tc(CO)$_3^+$ radiolabeling of the SAAC and SAAC II systems to form the desired ^{99m}Tc metal complexes was accomplished utilizing standard methodology [22] from the free acids or the protected *tert*-butyl ester derivatives. The radiolabeling was accomplished in two steps using commercially available IsoLink™ kits (Covidien) to form the $[^{99m}Tc(CO)_3(H_2O)_3]^+$ intermediate, which was neutralized and reacted with the appropriate SAAC or SAAC II system (Fig 2) at a concentration of 10^{-6} M in an equal volume mixture of acetonitrile and water in a sealed vial. The sealed vial was heated at 100 °C for 30 min and upon cooling the reaction was analyzed for purity via reverse-phase HPLC. The *tert*-butyl ester protecting groups were removed by treatment with 50% TFA in DCM for 45 min at room temperature. Upon completion of the deprotection, the reactions were concentrated on a rotary evaporator and purified by HPLC. The excess chelating agent was separated from the final ^{99m}Tc-products to the extent that <5% of the original 10^{-6} M chelate remained. The RCP was determined via HPLC and shown to be consistently ⩾90% pure.

2.5. Tissue distribution in LNCaP bearing mice

Uptake of radiolabeled complexes in LNCaP xenografts was performed according to published methods [23]. Briefly, LNCaP cells were trypsinized, counted, and suspended in a solution containing 50% Dulbecco's PBS (with 1 mg/mL D-glucose and 36 μg/mL sodium pyruvate) and 50% Matrigel (BD Biosciences, Franklin Lakes, NJ). Male NCr$^{nu/nu}$ mice were anesthetized by intraperitoneal injection of 0.5 mL Avertin (20 mg/mL) (Sigma-Aldrich, St. Louis, MO) then inoculated subcutaneously into the hind flank with 2×10^6 cells in a 0.25 mL suspension volume. Studies of tumor uptake were conducted when the tumors reached a size of 600–800 mm^3. Tissue distribution studies were conducted by administering, via the tail vein, a bolus injection of 2 μCi/mouse in a constant volume of 0.05 mL D-PBS. Groups of five animals were euthanized by asphyxiation with carbon dioxide at 1 h post injection. All tissues from Table 2, including the tumor were excised, weighed wet, transferred to plastic tubes and radioactivity assayed in an automated γ-counter (LKB Model 1282, Wallac Oy, Finland). Tissue time-radioactivity levels were expressed as % injected dose per gram tissue (%ID/g).

3. Results and discussion

We previously described the SAAC platform as a labeling technology for use with $Tc(CO)_3$ and $Re(CO)_3$, that has broad utility in radiochemical, fluorescent and dual modality (radio/fluorescent) molecular imaging [24,25]. This platform is particularly convenient for developing $^{99m}Tc(CO)_3$ – based radiolabeled small molecules. One limitation of the original SAAC platform which emphasized the $Tc(CO)_3$-dipyridyl complex as the prototype SAAC system, is the extremely hydrophobic nature of the radiolabeled complexes which often lead to high liver accumulation and/or hepatobiliary clearance of the bioconjugates derived from them [26]. Subsequently, we refined the platform to include imidazoles that would

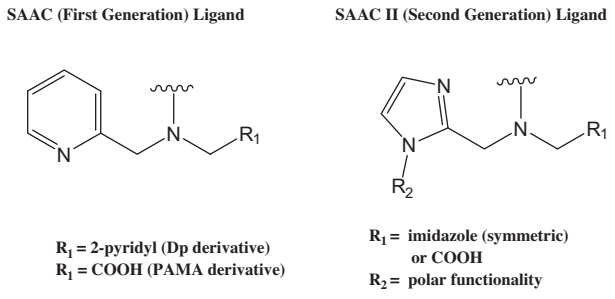

Fig. 1. General structure of the first (SAAC) and second generation (SAAC II) derived ligand systems.

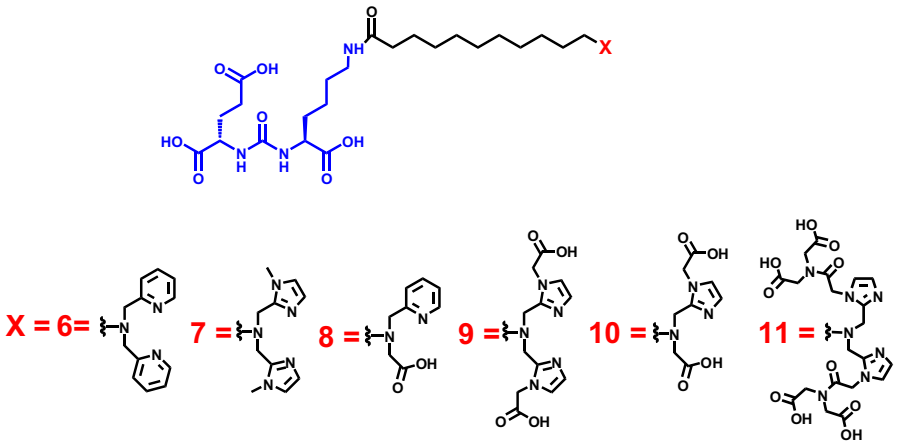

Fig. 2. Structures of the chelates employed to form the ^{99m}Tc-PSMA inhibitors derived from SAAC (**6**–**8**) and SAAC II (**9**–**11**) chelators.

allow pendant groups that would add charge and polarity to the overall metal-chelate complex independent of the coordinating donor atom set. This second generation SAAC, enabled more favorable pharmacokinetics and increased renal clearance of the ^{99m}Tc-labeled complexes. These changes in physicochemical properties yielded strong influence over pharmacokinetics and excretion. In addition, SAAC II systems could be successfully incorporated into the design of small ligands and low molecular weight peptides such as octreotide without detrimentally influencing receptor/enzyme interaction or pharmacokinetics and thus facilitate the development of novel ^{99m}Tc-labeled radiopharmaceuticals that possess more favorable biological distributions.

This was accomplished by derivatization of the imidazole rings [27] with polar carboxylic acid functional groups. The SAAC and SAAC II chelate systems were then examined on the Glu-urea-Lys-C11-X moiety (where X = SAAC or SAAC II derived chelate) for determination of their influence on the affinity and pharmacokinetic profiles of the complexes.

3.1. Chelate design

As illustrated below in Fig 1, first generation SAAC ligands incorporated either two pyridine rings or a pyridine and an acetic acid for **R1**. The design of the novel second generation bifunctional chelates explored the concept of increasing the water solubility and polarity of the chelate ring systems through the modification of the imidazole ring substituents, **R2**.

As previously reported, the homogenous polar derivatized imidazole SAAC II systems were prepared via the alkylation of the commercially available imidazole-2-carboxaldehyde with the desired alkyl halide to afford the *N*-substituted imidazole-2-carboxaldehyde analogs in moderate yields [20]. Reductive amination of 11-aminoundecanoic acid using sodium triacetoxyborohydride as the reducing agent produced the C11 derived SAAC/SAAC II intermediates **2** in good yield. Amide bond formation of **1** with **2** afforded the desired Glu-urea-Lys-C11-SAAC/SAAC II systems **3** in good yields as illustrated in Scheme 1. Subsequent treatment with the rhenium starting material $[NEt_4]_2[ReBr_3(CO)_3]$ followed by purification using C18 Sep Pak columns and subsequent deprotection with trifluoroacetic acid (TFA) afforded the desired series of metal complexes (**5**) in 5–60% yield.

The heterogeneous monoacetic acid SAAC ligand **8**, Fig 1 is smaller in size and can form less hindered complexes with a neutral uncharged metal center. The compounds in this series were prepared using the double reductive alkylation sequence on the appropriate protected amine followed by deprotection with TFA as previously described [16]. Deprotection employing trifluoroacetic acid (TFA) to yield the desired free ligand, **8**. Complexation to form the rhenium complex **8R** followed as described above for the homogenous SAAC and SAAC II systems.

3.2. In vitro binding and preliminary SAR of Glu-urea-X analogs

A series of Glu-urea-C11-SAAC/SAAC II heterodimers comprised of a Glu linked through a urea functionality to the α-amine of a modified Lys derivative were prepared as shown in Fig 2. The Glu residue contributes two of the three carboxylic acids important for binding to the PSMA active site [28–30]. The modified Lys residue contributes the third free carboxylic acid functionality and the ε-amine was utilized as the synthetic handle that led to the efficient synthesis of this series of C11 compounds which aided the rapid establishment of the SAR surrounding the chelator.

The compounds were evaluated in a competitive binding assay using ^{123}I-(*S*)-2-(3-((*S*)-1-carboxy-5-(4-iodobenzylamino) pentyl)ureido)pentanedioic acid or ^{123}I-DCIT as the radioligand for binding to PSMA on LNCaP cells.

One of the first Glu-urea-X heterodimers prepared and evaluated was **6**. The modest affinity of the rhenium complex **6R** (IC_{50} value 113 nM) shown in Table 1 demonstrated and confirmed that the Glu-urea-Lys recognition sequence could be derivatized with a metal chelate to afford active inhibitors with bulky metal centers extended away from the active site with a tether [31–33]. Similar binding affinity was observed with the rhenium analog of the *bis*-dimethylimidazole complex **7R** (IC_{50} value 183 nM) showing that the N-methyl imidazole appears to be a tolerated substitution for the 2-pyridyl ring in this series. The less bulky monoacetic acid derived neutral complex **8R** (IC_{50} value 696 nM) was significantly less potent possibly indicating a loss of a beneficial hydrophobic interaction with a secondary site on PSMA distant from the active site.

Table 1
Summary of *in vitro* cell binding data of the Re-Glu-urea-Lys-C11 derivatives.

Complex	Chelator (X)	IC_{50} (nM)
6	Di-pyridine-2-amine	113
7	Di-(*N*-methylimidazole)	183
8	Picoline-amine mono-acetic acid	696
9	Di-(*N*-carboxymethyl-imidazole) (CIM)	33
10	Mono-CIM-mono-acetic acid	10
11	Di-(*N*-dicarboxymethylamido-imidazole (TIM)	4

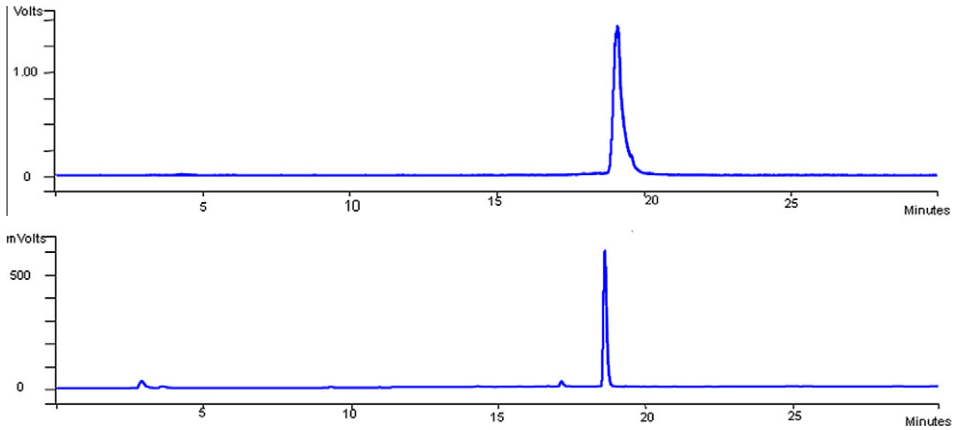

Fig. 3. Radiochromatograms of the ^{99m}Tc-**11** demonstrating >95% RCP (top), and the corresponding UV–Vis chromatogram of the rhenium complex used for identity confirmation (bottom).

The polar substituted SAAC II complexes **9R**–**11R** exhibited a substantial improvement in binding affinity for PSMA. The metal complexes, **9R** (IC_{50} value 33 nM), and **10R** at (IC_{50} value 10 nM) both have a pendant free carboxylic acid group attached to the imidazole donor rings. Although these complexes (**9R** and **10R**) were originally designed with the intention to drastically alter the tissue distribution and pharmacokinetic profiles of the conjugates, it appeared that they gained additional binding interactions, likely outside of the PSMA active site, due to the presence of the pendant carboxylic acid groups not present in the SAAC complexes **6R**–**8R**. Further increases in the number of pendant free acid functional groups through the use of the tetra-carboxy imidazole (**TIM**) chelator to form **11R** (IC_{50} value 4 nM) clearly demonstrated that the additional carboxylic acids appear to participate in favorable binding interactions that further improve affinity for PSMA.

3.3. Synthesis of ^{99m}Tc-SAAC/SAAC II ligands

Radiolabeling of the SAAC systems was accomplished on either the free acids or as the *tert*-butyl protected derivatives utilizing similar methodology, to form ^{99m}Tc-**6**–**11**, in excellent radiochemical yield. The $^{99m}Tc(CO)_3^+$ radiolabeling was accomplished in two steps using the commercially available IsoLink™ kits (Covidien) to generate the intermediate $[^{99m}Tc(CO)_3(H_2O)_3]^+$, which was reacted with the appropriate Glu-urea-Lys-C11-SAAC/SAAC II ligands (10^{-6} M) in an equal volume mixture of 1:1 acetonitrile: phosphate buffer in a sealed vial heated to 100 °C for 30 min. Upon cooling, the reaction was analyzed for purity via HPLC. RCP after deprotection and HPLC purification resulted in "no carrier added" products, with purity determined via HPLC to be consistently $\geqslant$90%, as shown for ^{99m}Tc-**11** in Fig. 3.

Tissue distribution of the series of ^{99m}Tc-complexes was evaluated in LNCaP tumor bearing mice at 1 h post injection. The results of the tissue distribution studies, Table 2, demonstrated a clear pattern present for all the original SAAC derived complexes ^{99m}Tc-**6**, ^{99m}Tc-**7**, ^{99m}Tc-**8**, with characteristically higher hepatobiliary uptake. Four of the complexes, ^{99m}Tc-**6**, ^{99m}Tc-**7**, ^{99m}Tc-**8** and ^{99m}Tc-**10** displayed >10%ID/g in the intestines at 1 h. These results were as predicted for ^{99m}Tc-**6**, ^{99m}Tc-**7**, and ^{99m}Tc-**8** with the very long C11 attached to the lipophilic cationic SAAC derived metal complexes. Surprisingly complex ^{99m}Tc-**10** also showed high intestinal uptake at 1 hour despite having a pendant carboxylic acid, which was intended to lower clearance via the hepatobiliary route. The unanticipated high intestinal uptake for ^{99m}Tc-**10** may be related to its neutral charge on the metal center or possessing only one pendant free carboxylic acid group may not be sufficient to compensate for the lipophilic character of the C11 backbone. It is clear that despite some of these complexes being rapidly cleared from the blood, most notably ^{99m}Tc-**7** and ^{99m}Tc-**10** (0.27 ± 0.05 and 0.23 ± 0.04%ID/g at 1 h, respectively) a significant portion of their excretion was via the hepatobiliary route, hindering the potential application of these chelators in the development of radiopharmaceuticals for prostate cancer. These limitations severely restrict the potential development of cancer imaging agents, where the ability to visualize metastatic lesions in the abdominal cavity would be confounded by the high background signal present in the liver and GI. Despite ^{99m}Tc-**10** possessing high affinity (IC_{50} value 10 nM), the tumor uptake for ^{99m}Tc-**10** was poor (3.29 ± 0.78%ID/g), possibly due to the lipophilic nature of the complex.

The ^{99m}Tc-SAAC complex, ^{99m}Tc-**9**, which contains two carboxylic acid functionalized imidazole rings exhibited very low liver

Table 2
Tissue distributions of ^{99m}Tc-Glu-urea-C11-SAAC/SAACII derived complexes at 1 h post injection in LNCaP xenograft mice.

Tissue	Complex					
	6	**7**	**8**	**9**	**10**	**11**
Blood	1.02 ± 1.19	0.27 ± 0.05	2.28 ± 2.38	1.06 ± 0.15	0.23 ± 0.04	0.99 ± 0.16
Heart	0.21 ± 0.04	0.13 ± 0.04	0.29 ± 0.24	1.39 ± 0.45	0.24 ± 0.04	0.25 ± 0.06
Lungs	0.5 ± 0.05	1.77 ± 2.55	0.91 ± 0.72	2.64 ± 0.47	0.75 ± 0.09	0.52 ± 0.03
Liver	2.13 ± 0.24	2.3 ± 1.41	2.54 ± 0.18	1.61 ± 0.17	3.73 ± 1.81	1.4 ± 0.23
Spleen	0.48 ± 0.23	0.34 ± 0.11	0.42 ± 0.34	15.68 ± 4.02	3.05 ± 1.67	1.44 ± 0.38
Kidneys	17 ± 2	23.8 ± 9.7	3.3 ± 1.3	147 ± 37	28 ± 6	61 ± 4
Stomach	0.61 ± 0.1	0.18 ± 0.11	0.87 ± 0.55	0.88 ± 0.2	1.74 ± 0.61	0.27 ± 0.12
Intestine	38.9 ± 2.2	18.9 ± 2.2	36.2 ± 9.8	6.59 ± 1.76	24.1 ± 3.1	0.66 ± 0.17
Sk. muscle	0.08 ± 0.05	0.04 ± 0.02	0.05 ± 0.04	0.57 ± 0.09	0.19 ± 0.06	0.72 ± 0.16
Tumor	1.24 ± 0.24	3.17 ± 0.82	0.72 ± 0.23	14.42 ± 5.93	3.29 ± 0.78	11.19 ± 3.13

Data are %ID/g, expressed as mean ± SD.

and gastrointestinal accumulation (1.61 ± 0.17 and 1.76 ± 0.57%ID/g at 1 h, respectively) and high tumor and kidney uptake (14.4 ± 5.93 and 147 ± 37% ID/g at 1 h, respectively). These properties are indicative of high affinity for PSMA and potential rapid clearance via the renal route. Interestingly, ^{99m}Tc-**9** demonstrated one of the highest tumor uptakes of any of the chelators examined. This is likely a combination of the high affinity for PSMA coupled with preferred renal clearance attributed to the polar negatively charged free carboxylic acids present in ^{99m}Tc-**9**.

Complex ^{99m}Tc-**11**, the *tetra*-carboxy containing imidazole analog also exhibited high tumor and kidney uptake, (11.19 ± 3.13 and 61 ± 4.0%ID/g at 1 h, respectively). Complex ^{99m}Tc-**11**, with four free pendant carboxylic acids available for binding to PSMA, displayed high affinity for PSMA likely due to secondary interactions with PSMA outside of the PSMA active site. The favorable high tumor uptake of ^{99m}Tc-**11** was complimented by a far superior overall tissue distribution compared to the other complexes evaluated. ^{99m}Tc-**11**, exhibited minimal liver uptake (1.4 ± 0.23%ID/g) and $\geqslant$tenfold less intestinal uptake (0.66 ± 0.17%ID/g) when compared to the other complexes studied. The nominal background was consistent throughout all the tissues examined and the low background led to very high signal-to-noise ratios demonstrating that ^{99m}Tc-**11** is the best preclinical candidate in this series.

4. Conclusions

The introduction of readily prepared aqueous solutions of ^{99m}Tc(CO)$_3$ by Alberto and Schubiger [14] stimulated our efforts to find a chelate suitable for taking advantage of the unique coordination chemistry of this metal core. Our ongoing research into the development of novel chelators for ^{99m}Tc(CO)$_3$ has lead to the development of a series of carboxylic acid substituted imidazole chelators (SAAC II) that offer significant improvements in overall clearance when compared to our original SAAC radiolabeling platform. The pharmacokinetic profile of the ^{99m}Tc(CO)$_3$-SAAC complex has been significantly altered through the design and synthesis of SAAC-II systems with the potential to enhance hydrophilicity and thereby increase renal clearance and diminish hepatobiliary accumulation and/or clearance. The benefit of the enhanced renal clearance and diminished hepatobiliary accumulation of the second generation ^{99m}Tc-SAAC II chelators was applied to the design of ^{99m}Tc-SAAC II derived PSMA inhibitor complexes, resulting in complexes with improved affinity for PSMA, and significant decrease in non-target tissue uptake. The results clearly demonstrated the dramatic influence the chelate can have on both affinity and pharmacokinetic properties. Future efforts will focus on the application of applying these SAAC II chelators to additional biologically relevant peptides and small molecules for the development of novel radiopharmaceuticals with improved disease targeting.

Acknowledgment

This work was supported in part by a Grant (J.W.B.) from the National Institutes of Health, Grant # 1R41A1054080-01.

Appendix A. Supplementary material

Supplementary data associated with this article can be found, in the online version, at http://dx.doi.org/10.1016/j.ica.2012.03.002.

References

[1] J. Steigman, W.C. Eckelman, ^{99m}Tc Chemistry as applied to medicine. Nuclear Science Series, National Research Council, National Academy Press, Washington, DC, 1992.
[2] C.F. Meares, M.K. Moi, H. Diril, D.L. Kukis, M.J. McCall, S.V. Deshpande, S.J. DeNardo, D. Snook, A.A. Epenetos, Br. J. Cancer Suppl. 10 (1990) 21.
[3] G. Mariani, M. Nicolini, H.W. Wagner, Technetium in Chemistry and Nuclear Medicine (and references within), vol. 1, Cortina International, Verona, 1983, p. 131.
[4] W.C. Eckelman, JACC Cardiovasc. Imaging 2 (3) (March 2009) 364.
[5] P. Richards, W.D. Tucker, S.C. Srivastava, Int. J. Appl. Radiat. Isot. 33 (10) (1982) 793.
[6] J.W. Babich, A.J. Fischman, Nucl. Med. Biol. 22 (1) (1995) 25.
[7] K. Verbeke, K. Snauwaert, B. Cleynhens, W. Scheers, A. Verbruggen, Nucl. Med. Biol. 27 (8) (2000) 769.
[8] E.A. Fragogeorgi, C. Zikos, E. Gourni, P. Bouziotis, M. Paravatou-Petsotas, G. Loudos, N. Mitsokapas, S. Xanthopoulos, M. Mavri-Vavayanni, E. Livaniou, A.D. Varvarigou, S.C. Archimandritis, Bioconjugate Chem. 20 (5) (2009) 856.
[9] P. Antunes, M. Ginj, H. Zhang, B. Waser, R.P. Baum, J.C. Reubi, H. Maecke, Eur. J. Nucl. Med. Mol. Imaging 34 (7) (2007) 982.
[10] E. Koumarianou, R. Mikołajczak, D. Pawlak, X. Zikos, P. Bouziotis, P. Garnuszek, U. Karczmarczyk, M. Maurin, S.C. Archimandritis, Nucl. Med. Biol. 36 (6) (2009 Aug) 591.
[11] M. Fani, L. Del Pozzo, K. Abiraj, R. Mansi, M.L. Tamma, R. Cescato, B. Waser, W.A. Weber, J.C. Reubi, H.R. Maecke, J. Nucl. Med. 52 (7) (2011) 1110.
[12] M.K. Levadala, S.R. Banerjee, K.P. Maresca, J.W. Babich, J. Zubieta, Synthesis 11 (2004) 1759.
[13] S.R. Banerjee, M.K. Levadala, N. Lazarova, L. Wei, J.F. Valliant, K.A. Stephenson, J.W. Babich, K.P. Maresca, J. Zubieta, Inorg. Chem. 41 (24) (2002) 6417.
[14] R. Alberto, A.P. Schubiger, J. Am. Chem. Soc. 120 (1998) 7987.
[15] R. Schibli, R. La Bella, R. Alberto, E. Garcia-Garayoa, K. Ortner, U. Abram, A.P. Schubiger, Bioconjugate Chem. 11 (2000) 345.
[16] K.P. Maresca, S.M. Hillier, F.J. Femia, C.N. Zimmerman, M.K. Levadala, S.R. Banerjee, J. Hicks, C. Sundararajan, J. Valliant, J. Zubieta, W. Eckelman, J.W. Babich, Bioconjugate Chem. 20 (8) (2009) 1625.
[17] M. Bartholomae, J. Valliant, K.P. Maresca, J.W. Babich, J. Zubieta, Chem. Commun. 5 (2009) 493.
[18] K.A. Stephenson, S.R. Banerjee, O.O. Sogbein, M.K. Levadala, N. McFarlane, D.R. Boreham, K.P. Maresca, J.W. Babich, J. Zubieta, J.F. Valliant, Bioconjugate Chem. 16 (5) (2005) 1189.
[19] K.A. Stephenson, S.R. Banerjee, N. McFarlane, D.R. Boreham, K.P. Maresca, J.W. Babich, J. Zubieta, J.F. Valliant, Can. J. Chem. 83 (12) (2005) 2060.
[20] K.P. Maresca, J.C. Marquis, S.M. Hillier, G. Lu, F.J. Femia, C.N. Zimmerman, W.C. Eckelman, J.L. Joyal, J.W. Babich, Bioconjugate Chem. 21 (6) (2010) 1032.
[21] K.P. Maresca, S.M. Hillier, F.J. Femia, D. Keith, C. Barone, J.L. Joyal, C.N. Zimmerman, A.P. Kozikowski, J.A. Barrett, W.C. Eckelman, J. Med. Chem. 52 (2) (2009) 347.
[22] R. Alberto, R. Schibli, R. Waibel, U. Abram, A.P. Schubiger, Coord. Chem. Rev. 190–192 (1999) 901.
[23] S.M. Hillier, K.P. Maresca, F.J. Femia, J.C. Marquis, C.A. Foss, N. Nguyen, C.N. Zimmerman, J.A. Barrett, W.C. Eckelman, M.G. Pomper, Cancer Res. 69 (17) (2009) 6932.
[24] S. James, K.P. Maresca, D.G. Allis, J.F. Valliant, W.C. Eckelman, J.W. Babich, J. Zubieta, Bioconjugate Chem. 17 (3) (2006) 579.
[25] K.A. Stephenson, J. Zubieta, S.R. Banerjee, M.K. Levadala, L. Taggart, L. Ryan, N. McFarlane, D.R. Boreham, K.P. Maresca, J.W. Babich, J.F. Valliant, Bioconjugate Chem. 15 (1) (2004) 128.
[26] K.A. Stephenson, S.R. Banerjee, T. Besanger, O.O. Sogbein, M.K. Levadala, N. McFarlane, J.A. Lemon, D.R. Boreham, K.P. Maresca, J.D. Brennan, J.W. Babich, J. Zubieta, J.F. Valliant, J. Am. Chem. Soc. 126 (28) (2004) 8598.
[27] K.P. Maresca, J.F. Kronauge, J. Zubieta, J.W. Babich, Inorg. Chem. Commun. 10 (12) (2007) 1409.
[28] A.P. Kozikowski, F. Nan, P. Conti, J.H. Zhang, E. Ramadan, T. Bzdega, B. Wroblewska, J.H. Neale, S. Pshenichkin, J.T. Wroblewski, J. Med. Chem. 44 (2001) 298.
[29] A. Oliver, A. Jayne, O. Wiest, P. Helquist, M.J. Miller, M. Tenniswood, Bioorg. Med. Chem. 11 (20) (2003) 4455.
[30] C. Barinka, M. Rovenska, P. Mlcochova, K. Hlouchova, A. Plechanovova, P. Majer, T. Tsukamoto, B.S. Slusher, J. Konvalinka, J. Lubkowski, J. Med. Chem. 50 (2007) 3267.
[31] S.R. Banerjee, C.A. Foss, M. Castanares, R.C. Mease, Y. Byun, J.J. Fox, J. Hilton, S.E. Lupold, A.P. Kozikowski, M.G. Pomper, J. Med. Chem. 51 (15) (2008) 4504.
[32] S.R. Banerjee, M. Pullambhatla, Y. Byun, S. Nimmagadda, C.A. Foss, G. Green, J.J. Fox, S.E. Lupold, R.C. Mease, M.G. Pomper, Angew. Chem., Int. Ed. 50 (39) (2011) 9167.
[33] C.A. Foss, R.C. Mease, H. Fan, Y. Wang, H.T. Ravert, R.F. Dannals, R. Olszewski, W.D. Heston, A.P. Kozikowski, M.G. Pomper, Clin. Canc. Res. 11 (2005) 4022.